Published in final edited form as:
Anat Rec (Hoboken). 2010 July ; 293(7): 1214–1226. doi:10.1002/ar.21152.

Ablation of systemic phosphate regulating gene fibroblast growth factor 23 (*Fgf23*) compromises the dentoalveolar complex

Ms. Emily Y. Chu, BS[1,2], **Dr. Hanson Fong, PhD**[3], **Dr. Fleur Blethen, DDS, MSD**[4], **Dr. Kevin A. Tompkins, DMD, PhD**[1,5], **Mr. Brian L. Foster, MS**[1,2], **Dr. Kuang-Dah Yeh, DDS, PhD, MSD**[2], **Dr. Kanako J. Nagatomo, DDS, PhD, MSD**[1], **Ms. Daisy Matsa-Dunn, BS**[1], **Dr. Despina Sitara, PhD**[6], **Dr. Beate Lanske, PhD**[6], **Dr. R. Bruce Rutherford, DDS, PhD**[2], and **Dr. Martha J. Somerman, DDS, PhD**[1,2]

Emily Y. Chu: eychu@u.washington.edu; Hanson Fong: hfong@u.washington.edu; Fleur Blethen: fblethen@gmail.com; Kevin A. Tompkins: kevin0318@yahoo.com; Brian L. Foster: blfoster@u.washington.edu; Kuang-Dah Yeh: yehkd592@u.washington.edu; Kanako J. Nagatomo: nagakana@u.washington.edu; Daisy Matsa-Dunn: daisy@dunns.info; Despina Sitara: despina_sitara@hsdm.harvard.edu; Beate Lanske: beate_lanske@hsdm.harvard.edu; R. Bruce Rutherford: rbruth@u.washington.edu; Martha J. Somerman: somerman@u.washington.edu

[1] Department of Periodontics, School of Dentistry, University of Washington, Seattle, WA, 98195, USA [2] Department of Oral Biology, School of Dentistry, University of Washington, Seattle, WA, 98195, USA [3] Department of Materials Science and Engineering, University of Washington, Seattle, WA, 98115, USA [4] Department of Endodontics, School of Dentistry, University of Washington, Seattle, WA, 98195, USA [5] Departments of Oral Biology and Implantology, Faculty of Dentistry, Chulalongkorn University, Bangkok Thailand [6] Department of Developmental Biology, Harvard School of Dental Medicine, Boston, MA, 02115, USA

Abstract

Fibroblast growth factor-23 (FGF23) is a hormone that modulates circulating phosphate (P_i) levels by controlling P_i reabsorption from the kidneys. When FGF23 levels are deficient, as in tumoral calcinosis patients, hyperphosphatemia ensues. We show here in a murine model that *Fgf23* ablation disrupted morphology and protein expression within the dentoalveolar complex. Ectopic matrix formation in pulp chambers, odontoblast layer disruption, narrowing of periodontal ligament space, and alteration of cementum structure were observed in histological and electron microscopy sections. Because serum P_i levels are dramatically elevated in *Fgf23*$^{-/-}$, we assayed for apoptosis and expression of members from the small integrin-binding ligand, N-linked glycoprotein (SIBLING) family, both of which are sensitive to elevated P_i *in vitro*. Unlike X-linked hypophosphatemic (*Hyp*) and wild-type (WT) specimens, numerous apoptotic osteocytes and osteoblasts were detected in *Fgf23*$^{-/-}$ specimens. Further, in comparison to *Hyp* and WT samples, decreased bone sialoprotein and elevated dentin matrix protein-1 protein levels were observed in cementum of *Fgf23*$^{-/-}$ mice. Additional dentin-associated proteins, such as dentin sialoprotein and dentin phosphoprotein, exhibited altered localization in both *Fgf23*$^{-/-}$ and *Hyp* samples. Based on these results, we propose that FGF23 and (P_i) homeostasis play a significant role in maintenance of the dentoalveolar complex.

*Corresponding Author: Dr. Martha J. Somerman, DDS, PhD, 1959 NE Pacific, Box 357444, University of Washington, Seattle, WA 98195-7444, Tel: (206) 685-2129; Fax: (206) 616-7478, somerman@u.washington.edu.

INTRODUCTION

Disruptions in serum phosphate (P_i) levels lead to skeletal and tooth abnormalities, which are evident in autosomal recessive hypophosphatemic rickets (ARHR) and X linked hypophosphatemic rickets (XLH) patients (Feng et al., 2006; Hardy et al., 1989; Pereira et al., 2004). Along with low P_i levels, these patients and murine homologues exhibit osteomalacia, expanded alveolar bone, increased predentin/dentin ratio, interglobular dentin, and enlarged pulp chambers (Abe et al., 1989; Feng et al., 2006; Liu et al., 2006; Murayama et al., 2000; Ye et al., 2004). The skeletal and tooth abnormalities associated with low P_i have been associated with an excess of serum fibroblast growth factor 23 (FGF23), a hormone discovered in patients with tumor induced osteomalacia (TIO), another P_i wasting disorder (ADHR_Consortium, 2000; Liu et al., 2006; Liu et al., 2008; Lorenz-Depiereux et al., 2006; Shimada et al., 2001; Sitara et al., 2004). FGF23 production has been localized predominantly to osteocytes, with lower levels noted in osteoblasts and cementoblasts (Quarles, 2003; Riminucci et al., 2003; Yoshiko et al., 2007).

FGF23 is also referred to as a phosphatonin because it decreases circulating P_i, joining ranks with classical hormonal P_i and calcium regulators 1,25-dihydroxyvitamin D_3 ($1,25(OH)_2D_3$) and parathyroid hormone (PTH). FGF23 reduces P_i by decreasing intestinal absorption via the sodium P_i transporter Npt2b, decreasing renal reabsorption via sodium P_i transporters Npt2a and Npt2c, as well as inhibition of 25-hydroxyvitamin D-1-α-hydroxylase (Jurutka et al., 2007; Larsson et al., 2004). 25-hydroxyvitamin D-1-α-hydroxylase is necessary for $1,25(OH)_2D_3$ activation, which, when suppressed, indirectly promotes Npt2a expression as FGF23 levels are lowered and PTH levels are increased(Sitara et al., 2006). Posttranslational modification is required for secretion of full-length FGF23. The enzyme uridine diphosphate-N-acetyl-α–D-galactosamine: polypeptide N-acetylgalactosaminyltransferase 3 (GALNT3) O-glycosylates FGF23, protecting it from proteolytic degradation (Ichikawa et al., 2007a; Ichikawa et al., 2009; Topaz et al., 2004). Further, in order for FGF23 to function, there is evidence that Klotho, a transmembrane protein expressed in the kidney, parathyroid, pituitary gland, and choroid plexus (Liu and Quarles, 2007; Xiao et al., 2004) is required to interact with cognate FGF receptors on cell surfaces and exert bioactivity on specific tissues (Memon et al., 2008; Nakatani et al., 2008). In situations where FGF23 function is diminished or ablated, hyperphosphatemia ensues as a consequence of excess P_i reabsorption. For example, one family of hyperphosphatemic disorders is hyperphosphatemic familial tumoral calcinosis (TC), which is subdivided into three types (Bergwitz and Juppner, 2009). Type I patients have deficient levels of full-length FGF23as a result of GALNT3 mutations (Garringer et al., 2007; Ichikawa et al., 2007a; Ichikawa et al., 2009; Topaz et al., 2004). Type II TC patients also have low full-length FGF23 levels, but these are attributed to mutations in FGF23 independent of GALNT3 function (Benet-Pages et al., 2005; Ichikawa et al., 2005; Masi et al., 2009). Type III TC patients have high levels of FGF23, but Klotho function is ablated, preventing FGF23 from functioning normally (Ichikawa et al., 2007b).

Research directed at elucidating the effects of systemic P_i dysregulation on mineralized tissues have been greatly aided by the use of homologous murine models associated with hypophosphatemia, i.e. ARHR (Dmp1-null mice), XLH (Hyp mouse), and hyperphosphatemia, i.e. TC (*Fgf23*$^{-/-}$, Klotho$^{-/-}$, and GALNT3 mutant mice) (Abe et al., 1989; Ichikawa et al., 2009; Kuro-o et al., 1997). Mutations in *dentin matrix protein-1* (*Dmp1*)and *phosphate-regulating gene with homologies to endopeptidases on the X-chromosome* (*Phex*), factors which may indirectly influence systemic P_i levels, cause ARHR and XLH in humans, respectively (Drezner, 2000; Farrow et al., 2007). Corresponding to human case reports, studies of hypophosphatemic Dmp1$^{-/-}$ and Hyp (Phex mutant) mice have identified dental defects primarily in the dentin, with minor changes in the cementum

(Fong et al., 2009; Ye et al., 2008). In our studies characterizing tooth development in *Hyp* mice, dentin defects were detected by histology, whereas the more subtle aberrant cementum phenotype required electron microscopy to be detected (Fong et al., 2009). In contrast, the teeth of hyperphosphatemic TC patients or mouse models (*Fgf23*$^{-/-}$, Klotho$^{-/-}$, and GALNT3 mutant mice) have not been studied extensively. Limited case reports of TC skeletal and tooth abnormalities noted calcification around major joints, hyperostosis, and ectopic calcification of the pulp chambers (Naikmasur et al., 2008; Witcher et al., 1989). Further, examination of incisors from Klotho$^{-/-}$ revealed dentin abnormalities (Suzuki et al., 2008). Because of the emphasis on dentin and pulp anomalies as a result of systemic P_i dysregulation in case studies, we hypothesized that hyperphosphatemia would lead to dramatic dentin and pulp abnormalities and minor, if any cementum alterations.

In order to put into context the effects of FGF23-mediated systemic P_i regulation on the dentoalveolar complex, we characterized the tooth phenotype of the hyperphosphatemic *Fgf23*$^{-/-}$ mouse, a homologue for TC Type II, using histological staining and electron microscopic analysis. To investigate mechanisms by which systemic P_i impacts mineralization, we used immunohistochemistry to determine expression patterns for selective bone/tooth markers in *Fgf23*$^{-/-}$ and *Hyp* mice. The *Hyp* mouse, while not a perfect inverse control of the *Fgf23*$^{-/-}$ mouse does feature high levels of circulating Fgf23 and is hypophosphatemic, providing a useful comparison regarding the roles of Fgf23 and P_i in tooth development. We report dramatic alterations in morphology, mineralization, and protein distribution in teeth and supporting structures as a consequence of *Fgf23* ablation.

MATERIALS AND METHODS

Animal maintenance and genotyping

Fgf23 heterozygote mouse breeding pairs were used to generate *Fgf23*$^{-/-}$ and wild type (WT) littermates for histological studies. Generation of these mice has been described previously (Sitara et al., 2004). Mice were housed in a specific pathogen free facility in 12 hr light-dark cycles and fed a standard rodent diet with access to water ad libitum. All animal studies were approved by the Institutional Animal Care and Use Committee, University of Washington (Seattle, WA, USA). Animals were genotyped with PCR amplified DNA extracted from tail snips using a RedExtract-N-Amp For Tissue kit (Sigma). The following PCR primers were used: *Fgf23* (5′ AGT GGA CGC TGG AGA ATG GCT ATG 3′ and 5′ CTG GGA AAG GGG CGA CAC C 3′, specific to Exon 3 of the wild-type); *Neo* (5′ AAG GTG AGA TGA CAG GAG ATC 3′ and 5′ GAT CGG CCA TTG AAC AAG ATG 3′, specific to *neomycin* of the mutant allele construct. The wild-type *Fgf23* product was 397 bp, while the mutant product was 310 bp. PCR cycling conditions used were: 94° C for 2 min; 37 cycles at 94° C for 40 sec, 60° C for 1 min, 72° C for 40 sec; 72° C for 10 min. Agarose gels were used to visualize PCR products.

Histology

Fgf23$^{-/-}$ and WT littermates were sacrificed at 23, 27, 33, 45, 61, and 75 days post-coital (dpc), where date of birth is about 19dpc. At least three samples from each time point and genotype were obtained. Sample heads were fixed in Bouin's overnight, and mandibles were dissected. Samples from 27dpc and later were demineralized (10% acetic acid, neutral buffered formalin, and sodium chloride), processed, and embedded for paraffin sectioning. 5μm buccolingual sections of the mandibular first molar were H&E stained. Images were obtained using a Nikon Eclipse E400 microscope camera system. In addition, 45dpc *Hyp* sections were prepared for comparison. *Hyp* samples were prepared as previously reported (Fong et al., 2009).

Electron Microscopy (EM)

Scanning electron microscopy (SEM) analyses were performed on lower right mandibles from 45dpcmice. Mandibles were sequentially dehydrated in 5%, 10%, 25%, 50%, 75%, and 100% aqueous ethanol solutions for 30 min each and mounted in room-temperature-cure epoxy (Allied High Tech Inc, Rancho Dominguez, CA). Subsequent preparation of epoxy-mounted specimens involved cutting the erupted incisor using a precision wafering saw (Buehler Ltd, Lake Bluff, IL) to expose the mesial surface of the first molar and the cross-section of the unerupted incisor. The cut surface was then ground further distally to expose the interior of the first molar using 600 then 1500 grit SiC papers, followed by smoothening via ultramicrotoming with a 45° angle diamond knife (Diatome, Inc., Hatfield, PA) fitted onto a MT 6000-XL ultra-microtome (Bal-Tec RMC, Inc., Tucson, AZ). All specimens were then mounted on SEM stubs, sputter coated with 5 nm of Pt for electron conductivity (SPI Supplies Inc, West Chester, PA), and imaged by an JSM7000F (JEOL-USA, Inc., Peabody, MA) SEM operating at 15kV in backscattering mode.

For transmission electron microscopy (TEM) analyses, mandibular molars still attached to alveolar bone were dehydrated and mounted following the same procedure as that for SEM. Mounted specimens were then ground to reveal the first molar interior. Without demineralizing, ultra-sections were prepared using a 45° angle diamond knife (Diatome, Inc., Hatfield, PA) fitted onto a MT 6000-XL ultra-microtome (Bal-Tec RMC, Inc., Tucson, AZ) and collected onto lacey-carbon coated Cu grids. TEM characterization was performed on a Philips EM420(FEI, Inc., Hillsborough, OR)microscope with a tungsten filament at 100keV.

Apoptosis assay

Apoptosis was detected using the TACS TdT Kit for terminal deoxynucleotidyl transferase-mediated deoxyuridinetriphosphate nick end-labeling (TUNEL) per kit instructions and a rabbit anti-mouse antibody for Caspase-3 (using the procedures described in the following immunohistochemistry section).

Immunohistochemistry (IHC)

Tissues from 45dpc *Fgf23*$^{-/-}$, *Hyp*, and WT mice were selected for IHC. Antibodies against mouse proteins included: BSP, dentin phosphoprotein (DPP), dentin sialoprotein (DSP), and DMP1. The BSP antibody was a gift from Dr. Renny Franceschi (University of Michigan), the DPP antibody was a gift from Dr. Arthur Veis (Northwestern University), the DSP (LF-153) antibody was a gift from Dr. Larry Fisher (NIH), and the DMP1 antibodies were gifts from Dr. Chunlin Qin (Baylor College of Dentistry) and purchased from Takara. Positive reactions were detected with AEC (3-amino-9-ethylcarbazole) solution. Sections were counterstained with hematoxylin. Antibodies were evaluated with n≥3 *Fgf23*$^{-/-}$, *Hyp*, and WT samples.

RESULTS

Alveolar bone, pulp, and PDL are dramatically altered in Fgf23$^{-/-}$ molar teeth (Figure 1)

As a first step, to characterize the effects of Fgf23 ablation on the dentoalveolar complex, we conducted a histological developmental time course of the mandibular first molar. Days were selected to capture developmental time points of interest, i.e. before root formation (23dpc), initiation of root/cementum formation (27dpc), during root formation and tooth eruption (33 and 45dpc), and following closure of the apex (61 through 96dpc). Disruptions in the dentoalveolar complex of the hyperphosphatemic *Fgf23*$^{-\backslash -}$ mouse were first noted at 33dpc, and by 45dpc, marked disturbances were present in the periodontium (Fig. 1A′).

At 33dpc and subsequent time points in *Fgf23*$^{-/-}$ mice, mandibular bone volume surrounding the incisor and molar was greatly expanded compared to WT, a trend particularly evident at 45dpc (Figs. 1A vs. A′, B vs. B′). The buccal aspect of the alveolar bone proper of *Fgf23*$^{-/-}$ mice was more than twice the width compared to that of WT controls (Figs. 1A vs. A′, B vs. B′). The expansion of the alveolar bone is reminiscent of reports from *Hyp* mice (Fong et al., 2009), and a mandibular first molar section from the hypophosphatemic *Hyp* mouse at 45dpc is provided for comparison (1A″). Further, the alveolar bone of *Fgf23*$^{-/-}$ mice appeared to be composed predominantly of woven bone with a higher density of osteocytes when compared with WT tissue sections (Fig. 1B vs. B′). By 61dpc, numerous empty lacunae were visible in alveolar bone of *Fgf23*$^{-/-}$ tissues (arrowhead, Fig. 1E′).

By 45dpc, disruption of the odontoblast layer characterized by a loss of cell polarity was observed in molars of *Fgf23*$^{-/-}$ mice, while the cementum, dentin, and predentin of the mandibular first molars appeared comparable in *Fgf23*$^{-/-}$ vs. WT tissues (Fig. 1C vs. C′, arrow). This directly contrasts with the marked dentin and predentin abnormalities observed in *Hyp* teeth (Fig. A″). Additionally, an ectopic matrix had developed in pulp chambers of *Fgf23*$^{-/-}$ mice at 45dpc and became more apparent by 61dpc (Fig. 1D′, arrows).

Alterations were present in the periodontal ligament (PDL) region by 45dpc, most consistently at the lingual aspect of the mandibular first molar in the coronal third of the root. Furthermore, PDL width was markedly reduced compared to the WT, with disorientation and compression of the PDL fibers (Fig. 1C vs. 1C′). At 61dpc, the PDL space was narrowed, and areas of near ankylosis were observed between bone and cementum at the site of PDL disruption. Few fibers were noted in the scant space between bone and cementum (Fig. 1E′, arrow).

Fgf23$^{-/-}$ mice exhibit marked mineralization defects, including a cementum phenotype (Figure 2)

In order to assess the mineral content of the hyperphosphatemic *Fgf23*$^{-/-}$ compared to the WT specimens, backscatter scanning electron microscopy (SEM) analysis was used. In these 45dpc un-demineralized sections, image brightness serves as an indicator of high mineral content. Consistent with reports of a lower mineral density of long bones in *Fgf23*$^{-/-}$ mice (Sitara et al., 2004; Sitara et al., 2006), the alveolar bone in the *Fgf23*$^{-/-}$ was significantly darker compared to WT, likely reflecting a composition of primarily osteoid(Figs. 2A vs 2A ′). The mineral content was so severely reduced in *Fgf23*$^{-/-}$ mice that alveolar bone was difficult to visualize by SEM; thus, expansion of bone width was not as apparent in these images as in comparable histological sections. This accumulation of osteoid is similar to the *Hyp* mouse bone (Fig. 2A″), in which mineralization defects in the bone, dentin, and cementum have been documented (Abe et al., 1989; Abe et al., 1992; Fong et al., 2009). Representative images of *Hyp* dentin and cementum are also shown here for comparison.

In support of the histological findings (Fig. 1), the alveolar bone of *Fgf23*$^{-/-}$ mice appeared less organized, i.e. characteristic lamellar structure as noted in the WT specimens was not observed. Further, compared to WT bone, osteocytes in *Fgf23*$^{-/-}$ bone were present in greater numbers and exhibited abnormal morphology (Figs. 2B vs. B, arrows). In contrast, in *Hyp* sections, osteocytes appeared more comparable to WT in morphology, although they inhabited irregular, large lacunae (Figs. 2B vs. B″, arrows).

Confirming histological observations, the dentin of *Fgf23*$^{-/-}$ mice was similar to that of WT mice and different from the *Hyp* mouse, which exhibited disruption of the tubules (Figs. 2C, C′ vs. C″). However, *Fgf23*$^{-/-}$ molar roots did not have the clear separation noted between cementum and dentin in WT specimens (Fig. 2C′, D′ vs. C, D). Transmission electron

microscopy analysis suggested alteration of cementum structure in *Fgf23*$^{-/-}$ mice compared to WT (Fig. 2D′ vs. 2D). However, the deviation from normal cementum in *Fgf23*$^{-/-}$ teeth was not the same as reported for *Hyp* mice, although *Hyp* specimens did not exhibit a clear demarcation between dentin and cementum as well (Figs. 2C″, D″).

Incisors of Fgf23$^{-/-}$ mice displaydentin and enamel abnormalities (Figure 3)

Although the murine incisor does not have a human counterpart, examining the continuously erupting murine incisors allows for the visualization of long-term sustained Fgf23 loss on tooth development. At 23 and 27dpc, no obvious differences were detected in mandibular incisors of *Fgf23*$^{-/-}$ vs. WT mice (data not shown). By 33dpc, incisors of *Fgf23*$^{-/-}$ mice exhibited morphological changes, including distorted shape, i.e. triangular cross-section vs. elliptical in WT, as well as development of a cyst-like structure in the region normally occupied by enamel (Fig. 3A vs. A′). Additionally, by 33dpc, a mineralized tissue-like matrix originating from the labial dentin (“crown analogue”) was observed extending into the incisor pulp chamber, with cells entrapped within this matrix (Figs. 3A′). SEM analysis revealed defective mineralization with an abnormal rod patterning in enamel of *Fgf23*$^{-/-}$ mice (Fig. 3B vs. B′, arrow). By 61dpc, the cyst-like structure at the labial aspect was no longer present, and the enamel space was reduced (Fig. 3C vs. C′). The mineral-like tissue present in the pulp at 33 and 45dpc increased markedly to the point of nearly obliterating the pulp chamber (Fig. 3C′). The odontoblast layer was completely disrupted and cells did not form the characteristic discrete, polarized layer on the border of the dentin matrix (C vs. C′, inset). In contrast, high levels of circulating FGF 23 characteristic of *Hyp* mice did not result in any unique pattern for incisors vs. molars during development.

Fgf23$^{-/-}$ mice exhibit increased apoptotic cells in the mandible compared to WT (Figure 4)

We observed numerous empty lacunae in mandibular bone and abnormal morphology of *Fgf23*$^{-/-}$ osteocytes. Because increased apoptosis has been reported in skeletal cells stimulated by elevated P_i levels *in vitro* (Adams et al., 2001), we assayed for apoptosis. Numerous positive TUNEL (Fig. 4A′) and caspase-3 reactions (Fig. 4B′) were observed in the marrow spaces, osteoblasts, and osteocytes of the alveolar bone in the *Fgf23*$^{-/-}$ mice. In addition, positive reactions were observed in the cells entrapped in the ectopic matrix of the incisor (data not shown). In contrast, very few apoptotic cells were detected in the WT tissues (Figs. 4A, B). Hyp tissues also exhibited very few apoptotic cells (data not shown).

Loss of Fgf23 and mutations in Phex cause altered expression of extracellular matrix proteins (Figure 5, Table 1)

Members of the small integrin-binding ligand, N-linked glycoprotein (SIBLING) family of extracellular matrix proteins (Fisher and Fedarko, 2003)have been reported to influence systemic P_i levels as well as being responsive to calcium/P_i regulating hormones, e.g. DMP1 loss results in excess FGF23 and hypophosphatemia (Chaussain-Miller et al., 2007; Feng et al., 2006; Fisher and Fedarko, 2003). To investigate possible mechanisms resulting in the dentoalveolar phenotype in Fgf 23 $^{-/-}$ mice, described above, immunohistochemistry was used to assay expression for selected SIBLING proteins in *Fgf23*$^{-/-}$ vs. WT samples. Further, we contrasted ECM protein expression of *Fgf23*$^{-/-}$ mice with comparable *Hyp* tissues (data not published previously). A descriptive summary of the results are provided in Table 1.

Bone sialoprotein (BSP)—*BSP*, a positive regulator of mineral formation (Malaval et al., 2008; Qin et al., 2004), was localized to cementum and alveolar bone in WT and *Hyp* sections (Figs. 5A vs. A″). In corresponding *Fgf23*$^{-/-}$ tissues, cementum stained very weakly and sporadically for *BSP* (Fig. 5A′, arrow), suggesting an altered cementum

composition and mineralization consistent with changes noted in SEM and TEM analysis. Further, *BSP* was apparently absent in *Fgf23*$^{-/-}$ alveolar bone adjacent to the PDL, contrasting with the strong localized BSP in the region associated with open osteocyte lacunae (Fig. 5A′, arrowhead).

Dentin Matrix Protein-1 (DMP1)—*DMP1* is an important factor in maturation of osteoblasts into osteocytes, and is a regulator of osteocyte behavior (Qin et al., 2007; Rios et al., 2005). In WT, positive staining for DMP1 was primarily localized around osteocytes in alveolar bone, as previously reported (Fig. 5B) (Toyosawa et al., 2001). Alveolar bone of *Hyp* mice exhibited intense DMP1 staining in perilacunar regions, but in contrast, in *Fgf23*$^{-/-}$ bone, large regions of bone adjacent to PDL were intensely positive for DMP1 (Figs. 5B′, B″). Further, *DMP1* staining was present in high levels in mantle dentin and a cellular cementum of *Fgf23*$^{-/-}$ samples, but was not detected in comparable sections from either *Hyp* or WT mice. These results were verified using multiple DMP1 antibodies (sections shown in Fig. 5 were stained with a commercially available DMP1 antibody targeted towards the N-terminal region).

Dentin sialoprotein (DSP) and Dentin phosphoprotein (DPP)—Immunopositive reactions for *DSP* and *DPP*, both protein products of *Dspp* mRNA transcript (MacDougall et al., 1997), indicated a different pattern of deposition in *Fgf23*$^{-/-}$ vs. *Hyp* vs. WT tissues. In WT sections, *DSP* was detected in dentinal tubules and mantle dentin, whereas in *Fgf23*$^{-/-}$ sections, *DSP* staining was strong but dispersed in dentin, with a higher intensity in the mantle dentin region (Figs. 5C vs. C′, arrow). In *Hyp* tissues, significant *DSP* staining was not apparent in the dentinal tubules, and staining in the mantle dentin appeared weaker than in WT and *Fgf23*$^{-/-}$ tissues(Figs. 5C″ vs. 5C, 5C′). In WT tissues, *DPP* was present in the predentin/dentin mineralization front, mantle dentin, and in odontoblasts, with low levels in pulp (Fig. 5D). *DPP* was similarly localized in *Fgf23*$^{-/-}$ sections, robust staining in the mantle dentin compared to WT. *Hyp* mouse molars featured overall weak DPP staining, including staining in the mantle dentin and predentin (Figs. 5D vs. 5D′, 5D″).

DISCUSSION

We sought to delineate the influence of hyperphosphatemia on development and mineralization of the dentoalveolar complex using *Fgf23*$^{-/-}$ mice and contrasting with hypophosphatemic *Hyp* and WT (normal P_i levels) controls. Based on previous studies, we hypothesized that systemic P_i dysregulation would lead to dramatic dentin and pulp abnormalities and less marked cementum abnormalities. Unexpectedly, our findings only partially correlated with our hypothesized results. Although both *Fgf23*$^{-/-}$ and *Hyp* mice exhibit abnormal systemic P_i regulation, dentin was dramatically altered only in the hypophosphatemic *Hyp* mice, whereas cementum was altered in both *Hyp* and *Fgf23*$^{-/-}$ mice. Extracellular matrix protein composition was altered in *Fgf23*$^{-/-}$ and *Hyp* dentin, cementum, and bone vs. WT. In addition to expanded and hypomineralized alveolar bone in *Fgf23*$^{-/-}$ mice, increased and widespread osteocyte apoptosis was apparent. Altogether, these results indicate that development and maintenance of the dentoalveolar complex is sensitive to systemic P_i dysregulation.

Although loss of Fgf23 seemingly results in widespread detrimental effects, i.e. multiple organ atrophy (Sitara et al., 2004), the results here indicate that Fgf23 has specific effects on each mineralized tissue type. The oral cavity presents a unique opportunity to simultaneously observe four different types of mineralized tissue: bone, cementum, dentin, and enamel. In the dentoalveolar complex at the level of the mandibular first molar, dentin and bone defects were the most conspicuous alterations (i.e. readily detected with H&E) in *Hyp* mice, whereas bone expansion coupled with PDL narrowing were the most apparent in

Fgf23$^{-/-}$ mice (Fig. 1). In both *Hyp* and *Fgf23*$^{-/-}$ specimens, cementum aberrations were not detectable by histology, but alterations in mineral density were observed using high magnification SEM and TEM (Fig. 2). Our observations here, as well as the globular cementum phenotype observed in *Hyp* mice, suggest that processes such as PDL maintenance and cementogenesis may be altered subsequent to P_i dysregulation, though the mechanism remains unknown. Additionally, studies on mice with loss of progressive ankylosis protein (ANK), ectonucleotide pyrophosphatase/phosphodiesterase 1 (ENPP1), or tissue non-specific alkaline phosphatase (TNAP) function have demonstrated sensitivity of cementum to dysregulation of P_i/PP_i homeostasis (Beertsen et al., 1999; Groeneveld et al., 1995; Millan et al., 2008; Nociti et al., 2002; van den Bos et al., 2005). Ank and Enpp1 mutant mice exhibit a marked hypercementosis phenotype, whereas Tnap mutants have cementum aplasia/hypoplasia resulting in exfoliation of teeth. Although these cementum alterations are a likely consequence of a microenvironmental P_i/PP_i ratio imbalance, these studies, along with the results presented here on systemic P_i dysregulation, indicate the importance of proper P_i regulation for formation of a normal dentoalveolar complex.

Alterations in protein expression described here suggest further roles for P_i and/or regulators of P_i metabolism on mineralized tissues of the oral cavity (summarized in Table 1). SIBLING proteins, extracellular matrix proteins found in dentin, cementum, and bone (D'Errico et al., 1997;Fisher et al., 2001;Fisher and Fedarko, 2003;Hunter and Goldberg, 1994;Hunter et al., 1996;Papagerakis et al., 2002;Qin et al., 2004;Rosen, 2008), exhibited altered expression in hypophosphatemic *Hyp* and hyperphosphatemic *Fgf23*$^{-/-}$ samples. BSP is a marker of bone and cementum, involved in osteoblast and cementoblast differentiation, and has roles in matrix mineralization (Bianco et al., 1993;Chen et al., 1992;D'Errico et al., 1997;Hunter and Goldberg, 1994;Hunter et al., 1996;Malaval et al., 2008). Notably, in cementoblasts, BSP mRNA transcription has been demonstrated to be down regulated in response to exogenous P_i *in vitro*, which parallels the sparse staining in the cementum of hyperphosphatemic *Fgf23*$^{-/-}$ mice (Foster et al., 2006;Rutherford et al., 2006). Moreover, *BSP* in *Fgf23*$^{-/-}$ alveolar bone region was characterized by areas of relatively heavy staining and areas with no apparent *BSP* present. Reductions in mineral markers such as BSP may reflect disrupted cell function or unregulated matrix synthesis by osteoblasts.

Interestingly, whereas BSP was down regulated in *Fgf23*$^{-/-}$ cementum and bone, DMP1 was up regulated. Further, regarding location of staining in the alveolar bone, DMP1 and BSP staining appeared to be inverses of each other in the hyperphosphatemic *Fgf23*$^{-/-}$ mouse. There are no studies demonstrating a feedback relationship between BSP and DMP1, and thus while speculative, the findings reported here suggest a common regulatory factor. Increased *DMP1* expression in *Fgf23*$^{-/-}$ samples correlated with *in vitro* studies on cementoblasts demonstrating increased mRNA transcripts for DMP1 in response to elevated P_i, suggesting that the elevated levels of DMP1 seen in *Fgf23*$^{-/-}$ tissues may be related directly to or regulated by high P_i levels (Foster et al., 2006; Rutherford et al., 2006). In bone, DMP1 was localized around osteocytes in WT samples, but was found in the extracellular matrix of *Fgf23*$^{-/-}$ and *Hyp* tissues. The increase in DMP1 staining in *Hyp* mice suggests local effects occurring independent of serum P_i and via mechanisms not completely understood. For example, studies have shown that osteocytes respond to force by synthesizing DMP1, so the unexpected DMP1 expression increase in the hypophosphatemic *Hyp* mice may be a consequence of amplified force transmission caused by a hypomineralized environment (Harris et al., 2007).

DMP1 has been reported to act as a nucleator of hydroxyapatite and is known to be required for skeletal development as well as dentinogenesis, as indicated by a reduced rate of dentin apposition and disruption in organization of dentinal tubules in *Dmp1*$^{-/-}$ mice (He et al.,

2003a; b; Lu et al., 2007; Tartaix et al., 2004; Ye et al., 2004). *Dmp1*$^{-/-}$ mice exhibit a tooth and bone phenotype remarkably similar to *Hyp* mice, including increased circulating levels of FGF23. A feedback loop between DMP1 and FGF23 has been proposed (Liu et al., 2008; Strom and Juppner, 2008). In light of this, increased DMP1 protein observed here in *Fgf23*$^{-/-}$ mice may in part contribute to the notable increase in alveolar bone volume and in ectopic extracellular matrix formation in the pulp region. Further, DMP1 regulates *Dspp* mRNA expression (Narayanan et al., 2006), which gives rise to DSP and DPP proteins (MacDougall et al., 1997). DSP and DPP exhibited altered localization in *Hyp* and *Fgf23*$^{-/-}$ mice. DSP and DPP have important roles in dentin mineralization and possibly in mineralization of other matrices (Baba et al., 2004; Hao et al., 2004; Qin et al., 2002; Qin et al., 2003a; Qin et al., 2003b; Sreenath et al., 2003). Thus, changes in localization and expression of *DMP1*, *DSP* and *DPP* possibly contribute to the ectopic matrix formation in *Fgf23*$^{-/-}$ mice, dentin mineralization abnormalities in *Hyp* mice, and the accumulation of osteoid in both *Hyp* and *Fgf23*$^{-/-}$ mice.

The alterations noted in the dentoalveolar complex of *Fgf23*$^{-/-}$ are consistent with case studies of TC patients and other hyperphosphatemic animal models. Reports of tumoral calcinosis patients, who have deficient FGF23 and elevated phosphate levels, include dystrophic pulp calcification, root dilacerations, and thistle shaped pulps (Dumitrescu et al., 2009; Naikmasur et al., 2008; Witcher et al., 1989). Further, *Klotho*$^{-/-}$ mice exhibit a nearly identical physical and biochemical phenotype to *Fgf23*$^{-/-}$ mice (e.g. elevated P_i and $1,25(OH)_2D_3$ levels) although Fgf23 levels in *Klotho*$^{-/-}$ mice are elevated (Kuro-o et al., 1997; Kuro-o, 2006; Memon et al., 2008). The dental aberrations noted in *Fgf23*$^{-/-}$ mice were similar to reports of increased apoptotic reactions and marked disturbances in odontoblasts, predentin, and dentin of incisors in *Klotho*$^{-/-}$ mice (Suzuki et al., 2005). In addition to P_i (Adams and Shapiro, 2003), apoptosis is induced by $1,25(OH)_2D_3$ (Medici et al., 2008), suggesting that at least some of the bone alterations in *Fgf23*$^{-/-}$ mice may be attributed to both elevated P_i and $1,25(OH)_2D_3$. Hyp/Klotho$^{-/-}$ and Hyp/*Fgf23*$^{-/-}$ compound mutants are also hyperphosphatemic with elevated $1,25(OH)_2D_3$ levels, demonstrating the importance of Fgf23 and Klotho in the pathology of hypophosphatemic rickets (Liu et al., 2006; Nakatani et al., 2009; Sitara et al., 2004). Our results, when considered alongside the similar tooth phenotype of the *Klotho*$^{-/-}$ mice, support the concept that klotho-FGF23 interactions are required for FGF23 to activate downstream events linked to controlling P_i metabolism in order to maintain a healthy dentoalveolar complex.

Considering data from this and other studies designed to define the key factors controlling P_i metabolism, it is important to recognize the intimate linkage of the hormones associated with the parathyroid-kidney-bone and tooth axis and when one of the three major hormones, i.e. PTH, $1,25(OH)_2D_3$, or FGF23is perturbed, all of these hormones and the downstream products they regulate are impacted. For example, in addition to being hyperphosphatemic, the *Fgf23*$^{-/-}$ mouse exhibits, hypercalcemia, hypoparathyrodisim, and hypervitamatosis D (Liu et al., 2006; Sitara et al., 2004). When either loss of 1-α hydroxylase or the $1,25(OH)_2D_3$ receptor is superimposed on loss of *FGF23*, hyperphosphatemia is reversed to hypophosphatemia and soft tissue calcifications are not observed (Hesse et al., 2007; Sitara et al., 2006). This outcome suggests elevated $1,25(OH)_2D_3$ levels play an important role in the mineralization defects characterizing *Fgf23*$^{-/-}$ mice (Shimada et al., 2004; Sitara et al., 2004). Additionally, the tooth phenotype in humans and animals lacking functional $1,25(OH)_2D_3$ included mineralization defects consistent with histological descriptions of the tooth phenotype in *Hyp* mice and XLH patients. Mice lacking $1,25(OH)_2D_3$ receptor expression displayed thin incisor dentin, enlarged pulp chambers, as well as widened and irregular predentin (Zhang et al., 2007). Thus, possible downstream effects of $1,25(OH)_2D_3$ in conjunction with FGF23 and P_i alterations will need to be investigated.

In the hypophosphatemic *Hyp* and the hyperphosphatemic *Fgf23*$^{-/-}$ mice, mineralization defects were first observed in 33dpc samples, suggesting a stage-specific role for *FGF23*. At early stages of development, *Fgf23* expression is normally low, indicating a minimal role in early developing tissues (Yoshiko et al., 2007). This is supported by lack of bone and teeth phenotypes at embryonic and early developmental ages, but an alternate explanation would be that the "normal" hormonal milieu that *Fgf23*$^{-/-}$ pups experience in utero protects against the inborn Fgf23 deficiency. With development of the mouse mandibular first molar completed by 45dpc, any detected changes in molar tissues from *Fgf23*$^{-/-}$ mice would likely be more homeostatic than developmental. In contrast, the mouse incisor is in a state of continuous development and eruption. Although the murine incisor does not have a human counterpart, examining murine incisors allows for the visualization of developmental processes completed by the molars prior to significant FGF23 expression. The presence of various stages of tooth development simultaneously is one possible explanation for the prominent incisor phenotype, including enamel defects, not seen in the molars. Further, we reported an improvement in *Hyp* dentin with time, suggesting a decreased role for FGF23 with age (Fong et al., 2009). Corroborating evidence includes findings that FGF23 expression may be suppressed in older tissues (Liu et al., 2007). Because the lifespan of *Fgf23*$^{-/-}$ mice is severely reduced (Sitara et al., 2004), we were unable to determine the effects of *Fgf23* ablation on older ages. Nonetheless, the marked alterations in the dentoalveolar complex illustrate profound effects of Fgf23 loss, indicating that FGF23 has a significant impact on development and maintenance of healthy teeth and supporting structures.

CONCLUDING REMARKS

Fgf23 ablation dramatically altered morphology and matrix composition of dentin, bone, and cementum. Current data, including our studies described here, highlight the complexity of positive and negative feedback interactions among these homeostatic factors, e.g. in addition to the influence of FGF23 and PHEX, P_i and $1,25(OH)_2D_3$ are regulated by other factors including calcium levels and PTH. Although direct and indirect effects on development of mineralized tissues are difficult to separate, the importance of further investigation to define regulators of P_i homeostasis is clear. The significant similarities between the Fgf 23 $^{-/-}$ in mice and humans in terms of bone pathology, coupled with the added knowledge from our studies may lead to more accurate diagnosis of phosphate metabolism disorders. Understanding the roles (s) for FGF23 in control of the dentoalveolar complex may lead to new approaches for developing more effective treatments for disorders in phosphate metabolism than those used at present.

Acknowledgments

The authors would like to thank the following for their contributions to this work: Dr. Ayu Murakami in the Somerman Lab, and support from the Departments of Periodontics and Oral Biology at the University of Washington School of Dentistry. This work was supported by NIH/NIDCR DE15109 (MJS), T32DE07132, and NIH/NIDDK DK073944 (BL).

Funding sources: NIH/NIDCR DE15109 (MJS), T32DE07132, NIH/NIDDK DK073944(BL)

References

Abe K, Ooshima T, Masatomi Y, Sobue S, Moriwaki Y. Microscopic and crystallographic examinations of the teeth of the X-linked hypophosphatemic mouse. J Dent Res. 1989; 68(11): 1519–24. [PubMed: 2584519]

Abe K, Masatomi Y, Nakajima Y, Shintani S, Moriwaki Y, Sobue S, et al. The occurrence of interglobular dentin in incisors of hypophosphatemic mice fed a high-calcium and high-phosphate diet. J Dent Res. 1992; 71(3):478–83. [PubMed: 1573080]

Adams CS, Mansfield K, Perlot RL, Shapiro IM. Matrix regulation of skeletal cell apoptosis. Role of calcium and phosphate ions. J Biol Chem. 2001; 276(23):20316–22. [PubMed: 11278303]

Adams CS, Shapiro IM. Mechanisms by which extracellular matrix components induce osteoblast apoptosis. Connect Tissue Res. 2003; 44(Suppl 1):230–9. [PubMed: 12952203]

ADHR_Consortium. Autosomal dominant hypophosphataemic rickets is associated with mutations in FGF23. Nat Genet. 2000; 26(3):345–8. [PubMed: 11062477]

Baba O, Qin C, Brunn JC, Jones JE, Wygant JN, McIntyre BW, et al. Detection of dentin sialoprotein in rat periodontium. Eur J Oral Sci. 2004; 112(2):163–70. [PubMed: 15056114]

Beertsen W, VandenBos T, Everts V. Root development in mice lacking functional tissue non-specific alkaline phosphatase gene: inhibition of acellular cementum formation [In Process Citation]. J Dent Res. 1999; 78(6):1221–9. [PubMed: 10371245]

Benet-Pages A, Orlik P, Strom TM, Lorenz-Depiereux B. An FGF23 missense mutation causes familial tumoral calcinosis with hyperphosphatemia. Hum Mol Genet. 2005; 14(3):385–90. [PubMed: 15590700]

Bergwitz C, Juppner H. Disorders of Phosphate Homeostasis and Tissue Mineralisation. Endocr Dev. 2009; 16:133–156. [PubMed: 19494665]

Bianco P, Riminucci M, Bonucci E, Termine JD, Robey PG. Bone sialoprotein (BSP) secretion and osteoblast differentiation: relationship to bromodeoxyuridine incorporation, alkaline phosphatase, and matrix deposition. J Histochem Cytochem. 1993; 41(2):183–91. [PubMed: 8419458]

Chaussain-Miller C, Sinding C, Septier D, Wolikow M, Goldberg M, Garabedian M. Dentin structure in familial hypophosphatemic rickets: benefits of vitamin D and phosphate treatment. Oral Dis. 2007; 13(5):482–9. [PubMed: 17714351]

Chen J, Shapiro HS, Sodek J. Developmental expression of bone sialoprotein mRNA in rat mineralized connective tissues. J Bone Miner Res. 1992; 7(8):987–97. [PubMed: 1442213]

D'Errico JA, MacNeil RL, Takata T, Berry J, Strayhorn C, Somerman MJ. Expression of bone associated markers by tooth root lining cells, in situ and in vitro. Bone. 1997; 20(2):117–26. [PubMed: 9028535]

Drezner MK. PHEX gene and hypophosphatemia. Kidney Int. 2000; 57(1):9–18. [PubMed: 10620182]

Dumitrescu CE, Kelly MH, Khosravi A, Hart TC, Brahim J, White KE, et al. A case of familial tumoral calcinosis/hyperostosis-hyperphosphatemia syndrome due to a compound heterozygous mutation in GALNT3 demonstrating new phenotypic features. Osteoporos Int. 2009; 20(7):1273–8. [PubMed: 18982401]

Farrow EG, Davis SI, Ward LM, White KE. The role of DMP1 in autosomal recessive hypophosphatemic rickets. J Musculoskelet Neuronal Interact. 2007; 7(4):310–2. [PubMed: 18094488]

Feng JQ, Ward LM, Liu S, Lu Y, Xie Y, Yuan B, et al. Loss of DMP1 causes rickets and osteomalacia and identifies a role for osteocytes in mineral metabolism. Nat Genet. 2006

Fisher LW, Torchia DA, Fohr B, Young MF, Fedarko NS. Flexible structures of SIBLING proteins, bone sialoprotein, and osteopontin. Biochem Biophys Res Commun. 2001; 280(2):460–5. [PubMed: 11162539]

Fisher LW, Fedarko NS. Six genes expressed in bones and teeth encode the current members of the SIBLING family of proteins. Connect Tissue Res. 2003; 44(Suppl 1):33–40. [PubMed: 12952171]

Fong H, Chu EY, Tompkins KA, Foster BL, Sitara D, Lanske B, et al. Aberrant cementum phenotype associated with the hypophosphatemic hyp mouse. J Periodontol. 2009; 80(8):1348–54. [PubMed: 19656036]

Foster BL, Nociti FH Jr, Swanson EC, Matsa-Dunn D, Berry JE, Cupp CJ, et al. Regulation of cementoblast gene expression by inorganic phosphate in vitro. Calcif Tissue Int. 2006; 78(2):103–12. [PubMed: 16467974]

Garringer HJ, Mortazavi SM, Esteghamat F, Malekpour M, Boztepe H, Tanakol R, et al. Two novel GALNT3 mutations in familial tumoral calcinosis. Am J Med Genet A. 2007; 143A(20):2390–6. [PubMed: 17853462]

Groeneveld MC, Everts V, Beertsen W. Alkaline phosphatase activity in the periodontal ligament and gingiva of the rat molar: its relation to cementum formation. J Dent Res. 1995; 74(7):1374–81. [PubMed: 7560388]

Hao J, Zou B, Narayanan K, George A. Differential expression patterns of the dentin matrix proteins during mineralized tissue formation. Bone. 2004; 34(6):921–32. [PubMed: 15193538]

Hardy DC, Murphy WA, Siegel BA, Reid IR, Whyte MP. X-linked hypophosphatemia in adults: prevalence of skeletal radiographic and scintigraphic features. Radiology. 1989; 171(2):403–14. [PubMed: 2539609]

Harris SE, Gluhak-Heinrich J, Harris MA, Yang W, Bonewald LF, Riha D, et al. DMP1 and MEPE expression are elevated in osteocytes after mechanical loading in vivo: theoretical role in controlling mineral quality in the perilacunar matrix. J Musculoskelet Neuronal Interact. 2007; 7(4):313–5. [PubMed: 18094489]

He G, Dahl T, Veis A, George A. Dentin matrix protein 1 initiates hydroxyapatite formation in vitro. Connect Tissue Res. 2003a; 44(Suppl 1):240–5. [PubMed: 12952204]

He G, Dahl T, Veis A, George A. Nucleation of apatite crystals in vitro by self-assembled dentin matrix protein 1. Nat Mater. 2003b; 2(8):552–8. [PubMed: 12872163]

Hesse M, Frohlich LF, Zeitz U, Lanske B, Erben RG. Ablation of vitamin D signaling rescues bone, mineral, and glucose homeostasis in Fgf-23 deficient mice. Matrix Biol. 2007; 26(2):75–84. [PubMed: 17123805]

Hunter GK, Goldberg HA. Modulation of crystal formation by bone phosphoproteins: role of glutamic acid-rich sequences in the nucleation of hydroxyapatite by bone sialoprotein. Biochem J. 1994; 302(Pt 1):175–9. [PubMed: 7915111]

Hunter GK, Hauschka PV, Poole AR, Rosenberg LC, Goldberg HA. Nucleation and inhibition of hydroxyapatite formation by mineralized tissue proteins. Biochem J. 1996; 317(Pt 1):59–64. [PubMed: 8694787]

Ichikawa S, Lyles KW, Econs MJ. A novel GALNT3 mutation in a pseudoautosomal dominant form of tumoral calcinosis: evidence that the disorder is autosomal recessive. J Clin Endocrinol Metab. 2005; 90(4):2420–3. [PubMed: 15687324]

Ichikawa S, Guigonis V, Imel EA, Courouble M, Heissat S, Henley JD, et al. Novel GALNT3 mutations causing hyperostosis-hyperphosphatemia syndrome resultin low intact fibroblast growth factor 23 concentrations. J Clin Endocrinol Metab. 2007a; 92(5):1943–7. [PubMed: 17311862]

Ichikawa S, Imel EA, Kreiter ML, Yu X, Mackenzie DS, Sorenson AH, et al. A homozygous missense mutation in human KLOTHO causes severe tumoral calcinosis. J Clin Invest. 2007b; 117(9):2684–91. [PubMed: 17710231]

Ichikawa S, Sorenson AH, Austin AM, Mackenzie DS, Fritz TA, Moh A, et al. Ablation of the Galnt3 gene leads to low-circulating intact fibroblast growth factor 23 (Fgf23) concentrations and hyperphosphatemia despite increased Fgf23 expression. Endocrinology. 2009; 150(6):2543–50. [PubMed: 19213845]

Jurutka PW, Bartik L, Whitfield GK, Mathern DR, Barthel TK, Gurevich M, et al. Vitamin D receptor: key roles in bone mineral pathophysiology, molecular mechanism of action, and novel nutritional ligands. J Bone Miner Res. 2007; 22(Suppl 2):V2–10. [PubMed: 18290715]

Kuro-o M, Matsumura Y, Aizawa H, Kawaguchi H, Suga T, Utsugi T, et al. Mutation of the mouse klotho gene leads to a syndrome resembling ageing. Nature. 1997; 390(6655):45–51. [PubMed: 9363890]

Kuro-o M. Klotho as a regulator of fibroblast growth factor signaling and phosphate/calcium metabolism. Curr Opin Nephrol Hypertens. 2006; 15(4):437–41. [PubMed: 16775459]

Larsson T, Marsell R, Schipani E, Ohlsson C, Ljunggren O, Tenenhouse HS, et al. Transgenic mice expressing fibroblast growth factor 23 under the control of the alpha1(I) collagen promoter exhibit growth retardation, osteomalacia, and disturbed phosphate homeostasis. Endocrinology. 2004; 145(7):3087–94. [PubMed: 14988389]

Liu S, Zhou J, Tang W, Jiang X, Rowe DW, Quarles LD. Pathogenic Role of FGF23 in Hyp Mice. Am J Physiol Endocrinol Metab. 2006

Liu S, Quarles LD. How fibroblast growth factor 23 works. J Am Soc Nephrol. 2007; 18(6):1637–47. [PubMed: 17494882]

Liu S, Tang W, Zhou J, Vierthaler L, Quarles LD. Distinct roles for intrinsic osteocyte abnormalities and systemic factors in regulation of FGF23 and bone mineralization in Hyp mice. Am J Physiol Endocrinol Metab. 2007; 293(6):E1636–44. [PubMed: 17848631]

Liu S, Zhou J, Tang W, Menard R, Feng JQ, Quarles LD. Pathogenic role of Fgf23 in Dmp1-null mice. Am J Physiol Endocrinol Metab. 2008; 295(2):E254–61. [PubMed: 18559986]

Lorenz-Depiereux B, Bastepe M, Benet-Pages A, Amyere M, Wagenstaller J, Muller-Barth U, et al. DMP1 mutations in autosomal recessive hypophosphatemia implicate a bone matrix protein in the regulation of phosphate homeostasis. Nat Genet. 2006; 38(11):1248–50. [PubMed: 17033625]

Lu Y, Ye L, Yu S, Zhang S, Xie Y, McKee MD, et al. Rescue of odontogenesis in Dmp1-deficient mice by targeted re-expression of DMP1 reveals roles for DMP1 in early odontogenesis and dentin apposition in vivo. Dev Biol. 2007; 303(1):191–201. [PubMed: 17196192]

MacDougall M, Simmons D, Luan X, Nydegger J, Feng J, Gu TT. Dentin phosphoprotein and dentin sialoprotein are cleavage products expressed from a single transcript coded by a gene on human chromosome 4. Dentin phosphoprotein DNA sequence determination. J Biol Chem. 1997; 272(2): 835–42. [PubMed: 8995371]

Malaval L, Wade-Gueye NM, Boudiffa M, Fei J, Zirngibl R, Chen F, et al. Bone sialoprotein plays a functional role in bone formation and osteoclastogenesis. J Exp Med. 2008; 205(5):1145–53. [PubMed: 18458111]

Masi L, Gozzini A, Franchi A, Campanacci D, Amedei A, Falchetti A, et al. A novel recessive mutation of fibroblast growth factor-23 in tumoral calcinosis. J Bone Joint Surg Am. 2009; 91(5): 1190–8. [PubMed: 19411468]

Medici D, Razzaque MS, Deluca S, Rector TL, Hou B, Kang K, et al. FGF-23-Klotho signaling stimulates proliferation and prevents vitamin D-induced apoptosis. J Cell Biol. 2008; 182(3):459–65. [PubMed: 18678710]

Memon F, El-Abbadi M, Nakatani T, Taguchi T, Lanske B, Razzaque MS. Does Fgf23-klotho activity influence vascular and soft tissue calcification through regulating mineral ion metabolism? Kidney Int. 2008

Millan JL, Narisawa S, Lemire I, Loisel TP, Boileau G, Leonard P, et al. Enzyme replacement therapy for murine hypophosphatasia. J Bone Miner Res. 2008; 23(6):777–87. [PubMed: 18086009]

Murayama T, Iwatsubo R, Akiyama S, Amano A, Morisaki I. Familial hypophosphatemic vitamin D-resistant rickets: dental findings and histologic study of teeth. Oral Surg Oral Med Oral Pathol Oral Radiol Endod. 2000; 90(3):310–6. [PubMed: 10982952]

Naikmasur V, Guttal K, Bhargava P, Burde K, Sattur A, Nandimath K. Tumoral calcinosis with dental manifestations--a case report. Dent Update. 2008; 35(2):134–6. 138. [PubMed: 18426167]

Nakatani T, Sarraj B, Ohnishi M, Densmore MJ, Taguchi T, Goetz R, et al. In vivo genetic evidence for klotho-dependent, fibroblast growth factor 23 (Fgf23) -mediated regulation of systemic phosphate homeostasis. Faseb J. 2008

Nakatani T, Ohnishi M, Razzaque MS. Inactivation of klotho function induces hyperphosphatemia even in presence of high serum fibroblast growth factor23 levels in a genetically engineered hypophosphatemic (Hyp) mouse model. Faseb J. 2009

Narayanan K, Gajjeraman S, Ramachandran A, Hao J, George A. Dentin matrix protein 1 regulates dentin sialophosphoprotein gene transcription during early odontoblast differentiation. J Biol Chem. 2006; 281(28):19064–71. [PubMed: 16679514]

Nociti FH Jr, Berry JE, Foster BL, Gurley KA, Kingsley DM, Takata T, et al. Cementum: a phosphate-sensitive tissue. J Dent Res. 2002; 81(12):817–21. [PubMed: 12454094]

Papagerakis P, Berdal A, Mesbah M, Peuchmaur M, Malaval L, Nydegger J, et al. Investigation of osteocalcin, osteonectin, and dentin sialophosphoprotein in developing human teeth. Bone. 2002; 30(2):377–85. [PubMed: 11856645]

Pereira CM, de Andrade CR, Vargas PA, Coletta RD, de Almeida OP, Lopes MA. Dental alterations associated with X-linked hypophosphatemic rickets. J Endod. 2004; 30(4):241–5. [PubMed: 15085056]

Qin C, Brunn JC, Cadena E, Ridall A, Tsujigiwa H, Nagatsuka H, et al. The expression of dentin sialophosphoprotein gene in bone. J Dent Res. 2002; 81(6):392–4. [PubMed: 12097430]

Qin C, Brunn JC, Baba O, Wygant JN, McIntyre BW, Butler WT. Dentin sialoprotein isoforms: detection and characterization of a high molecular weight dentin sialoprotein. Eur J Oral Sci. 2003a; 111(3):235–42. [PubMed: 12786955]

Qin C, Brunn JC, Cadena E, Ridall A, Butler WT. Dentin sialoprotein in bone and dentin sialophosphoprotein gene expressed by osteoblasts. Connect Tissue Res. 2003b; 44(Suppl 1):179–83. [PubMed: 12952194]

Qin C, Baba O, Butler WT. Post-translational modifications of sibling proteins and their roles in osteogenesis and dentinogenesis. Crit Rev Oral Biol Med. 2004; 15(3):126–36. [PubMed: 15187031]

Qin C, D'Souza R, Feng JQ. Dentin matrix protein 1 (DMP1): new and important roles for biomineralization and phosphate homeostasis. J Dent Res. 2007; 86(12):1134–41. [PubMed: 18037646]

Quarles LD. FGF23, PHEX, and MEPE regulation of phosphate homeostasis and skeletal mineralization. Am J Physiol Endocrinol Metab. 2003; 285(1):E1–9. [PubMed: 12791601]

Riminucci M, Collins MT, Fedarko NS, Cherman N, Corsi A, White KE, et al. FGF-23 in fibrous dysplasia of bone and its relationship to renal phosphate wasting. J Clin Invest. 2003; 112(5):683–92. [PubMed: 12952917]

Rios HF, Ye L, Dusevich V, Eick D, Bonewald LF, Feng JQ. DMP1 is essential for osteocyte formation and function. J Musculoskelet Neuronal Interact. 2005; 5(4):325–7. [PubMed: 16340123]

Rosen CJ. Bone remodeling, energy metabolism, and the molecular clock. Cell Metab. 2008; 7(1):7–10. [PubMed: 18177720]

Rutherford RB, Foster BL, Bammler T, Beyer RP, Sato S, Somerman MJ. Extracellular phosphate alters cementoblast gene expression. J Dent Res. 2006; 85(6):505–9. [PubMed: 16723645]

Shimada T, Mizutani S, Muto T, Yoneya T, Hino R, Takeda S, et al. Cloning and characterization of FGF23 as a causative factor of tumor-induced osteomalacia. Proc Natl Acad Sci U S A. 2001; 98(11):6500–5. [PubMed: 11344269]

Shimada T, Kakitani M, Yamazaki Y, Hasegawa H, Takeuchi Y, Fujita T, et al. Targeted ablation of Fgf23 demonstrates an essential physiological role of FGF23 in phosphate and vitamin D metabolism. J Clin Invest. 2004; 113(4):561–8. [PubMed: 14966565]

Sitara D, Razzaque MS, Hesse M, Yoganathan S, Taguchi T, Erben RG, et al. Homozygous ablation of fibroblast growth factor-23 results in hyperphosphatemia and impaired skeletogenesis, and reverses hypophosphatemia in Phex-deficient mice. Matrix Biol. 2004; 23(7):421–32. [PubMed: 15579309]

Sitara D, Razzaque MS, St-Arnaud R, Huang W, Taguchi T, Erben RG, et al. Genetic ablation of vitamin D activation pathway reverses biochemical and skeletal anomalies in Fgf-23-null animals. Am J Pathol. 2006; 169(6):2161–70. [PubMed: 17148678]

Sreenath T, Thyagarajan T, Hall B, Longenecker G, D'Souza R, Hong S, et al. Dentin sialophosphoprotein knockout mouse teeth display widened predentin zone and develop defective dentin mineralization similar to human dentinogenesis imperfecta type III. J Biol Chem. 2003; 278(27):24874–80. [PubMed: 12721295]

Strom TM, Juppner H. PHEX, FGF23, DMP1 and beyond. Curr Opin Nephrol Hypertens. 2008; 17(4): 357–62. [PubMed: 18660670]

Suzuki H, Amizuka N, Oda K, Li M, Yoshie H, Ohshima H, et al. Histological evidence of the altered distribution of osteocytes and bone matrix synthesis in klotho-deficient mice. Arch Histol Cytol. 2005; 68(5):371–81. [PubMed: 16505583]

Suzuki H, Amizuka N, Oda K, Noda M, Ohshima H, Maeda T. Involvement of the klotho protein in dentin formation and mineralization. Anat Rec (Hoboken). 2008; 291(2):183–90. [PubMed: 18085632]

Tartaix PH, Doulaverakis M, George A, Fisher LW, Butler WT, Qin C, et al. In vitro effects of dentin matrix protein-1 on hydroxyapatite formation provide insights into in vivo functions. J Biol Chem. 2004; 279(18):18115–20. [PubMed: 14769788]

Topaz O, Shurman DL, Bergman R, Indelman M, Ratajczak P, Mizrachi M, et al. Mutations in GALNT3, encoding a protein involved in O-linked glycosylation, cause familial tumoral calcinosis. Nat Genet. 2004; 36(6):579–81. [PubMed: 15133511]

Toyosawa S, Shintani S, Fujiwara T, Ooshima T, Sato A, Ijuhin N, et al. Dentin matrix protein 1 is predominantly expressed in chicken and rat osteocytes but not in osteoblasts. J Bone Miner Res. 2001; 16(11):2017–26. [PubMed: 11697797]

van den Bos T, Handoko G, Niehof A, Ryan LM, Coburn SP, Whyte MP, et al. Cementum and dentin in hypophosphatasia. J Dent Res. 2005; 84(11):1021–5. [PubMed: 16246934]

Witcher SL Jr, Drinkard DW, Shapiro RD, Schow CE Jr. Tumoral calcinosis with unusual dental radiographic findings. Oral Surg Oral Med Oral Pathol. 1989; 68(1):104–7. [PubMed: 2666895]

Xiao NM, Zhang YM, Zheng Q, Gu J. Klotho is a serum factor related to human aging. Chin Med J (Engl). 2004; 117(5):742–7. [PubMed: 15161545]

Ye L, MacDougall M, Zhang S, Xie Y, Zhang J, Li Z, et al. Deletion of dentin matrix protein-1 leads to a partial failure of maturation of predentin into dentin, hypomineralization, and expanded cavities of pulp and root canal during postnatal tooth development. J Biol Chem. 2004; 279(18): 19141–8. [PubMed: 14966118]

Ye L, Zhang S, Ke H, Bonewald LF, Feng J. Periodontal breakdown in the dmp1 null mouse model of hypophosphatemic rickets. J Dent Res. 2008; 87(7):624–9. [PubMed: 18573980]

Yoshiko Y, Wang H, Minamizaki T, Ijuin C, Yamamoto R, Suemune S, et al. Mineralized tissue cells are a principal source of FGF23. Bone. 2007; 40(6):1565–73. [PubMed: 17350357]

Zhang X, Rahemtulla FG, MacDougall MJ, Thomas HF. Vitamin D receptor deficiency affects dentin maturation in mice. Arch Oral Biol. 2007; 52(12):1172–9. [PubMed: 17707333]

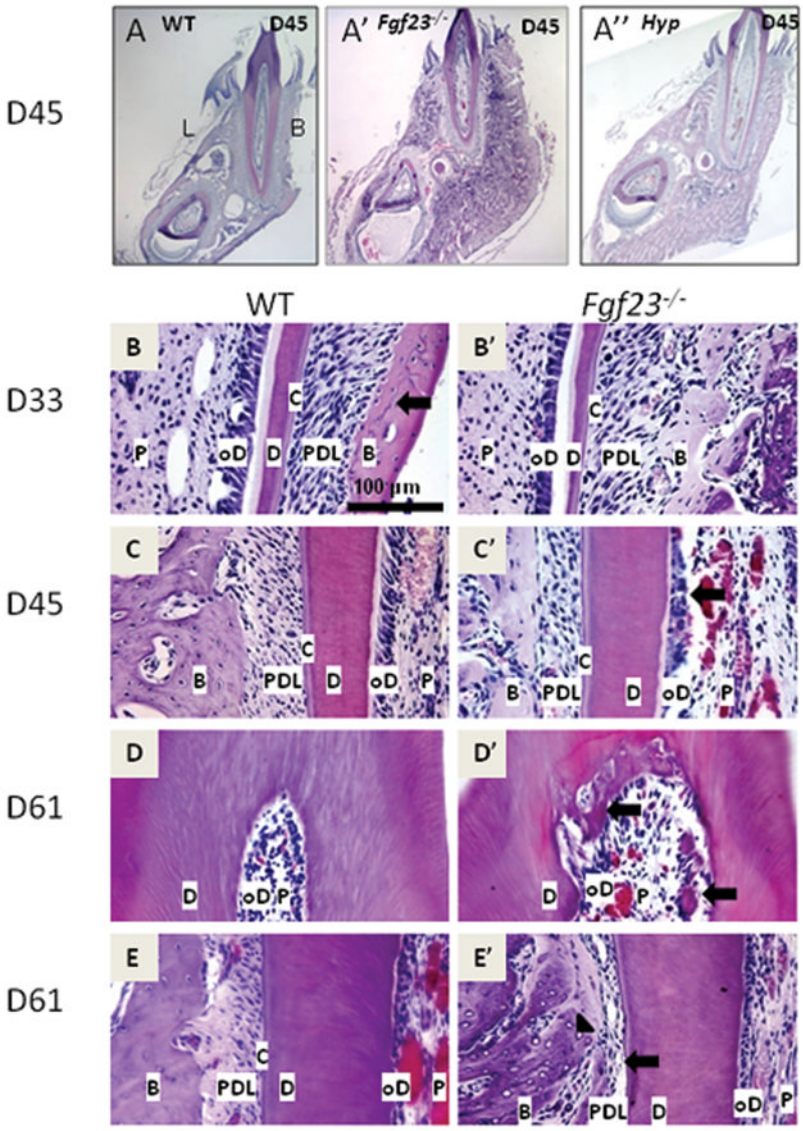

Figure 1. Mandibular molars of *Fgf23*$^{-/-}$ mice exhibit disruption of odontoblast layer and ectopic matrix deposition in pulp chambers

Representative H&E stained histological sections from mouse molars at 33, 45, and 61dpc (at least three samples from each age and genotype were evaluated). P=pulp, oD=odontoblasts, D=dentin, C=cementum, PDL=periodontal ligament, B=bone **(A)** Low magnifcation of WT buccolingual section. L and B signify lingual and buccal (labial), respectively. **(A′)** Low magnification of *Fgf23*$^{-/-}$ buccolingual section. Note increase in volume of the alveolar bone region in the *Fgf23*$^{-/-}$ mouse (A′) vs. WT. **(A″)** Low magnification of *Hyp* mouse buccolingual section. Note increase in volume of alveolar bone region compared to WT.**(B)** Buccal aspect of WT mandibular first molar at 33dpc. **(B′)** Buccal aspect of *Fgf23*$^{-/-}$ mandibular first molar at 33dpc. *Fgf23*$^{-/-}$ mice exhibited increased volume in the alveolar bone region. No clear differences were noted in the odontoblasts, predentin, dentin, cementum, and PDL in *Fgf23*$^{-/-}$ vs. WT. **(C, C′)** Lingual aspect of WT (1C) and *Fgf23*$^{-/-}$ (1C′) mandibular first molar at 45dpc. Compared to WT, the odontoblast layer in the *Fgf23*$^{-/-}$ mouse has lost its polarized nature (arrows), PDL width is reduced and fibers are slightly disorganized. **(D, D′)** Coronal region of *Fgf23*$^{-/-}$

mandibular first molar at 61dpc (1D′) compared to WT (1D). Note loss of polarization in the *Fgf23*$^{-/-}$ odontoblast layer compared to WT. Arrows indicate areas of ectopic matrix in the pulp chamber. **(E, E′)** Lingual aspect of WT (1E) and *Fgf23*$^{-/-}$ (1E′) mandibular first molars at 61dpc. Note near ankylosis (arrow) in the *Fgf23*$^{-/-}$ mouse. Also, many empty lacunae are visible in the bone of the *Fgf23*$^{-/-}$ mouse (arrowhead).

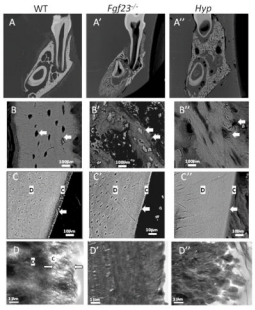

Figure 2. Fgf23$^{-/-}$ mice exhibit marked mineralization defects, including a cementum phenotype

Representative images from SEM and TEM analysis of 45dpc WT, *Fgf23*$^{-/-}$, and *Hyp* mandibular first molars and surrounding alveolar bone (At least three samples from each age and genotype were evaluated). D=dentin, C=cementum

(A, A′, A″) Cross section of *Fgf23*$^{-/-}$ (2A′) compared to WT (2A) and (2A″). **(B, B′, B″)** High magnification of alveolar bone region of *Fgf23*$^{-/-}$ (2B′) mice compared to WT (2B) and Hyp (2B″). Note inconsistent mineralization and abnormal osteocytes (arrow) in the *Fgf23*$^{-/-}$ bone (2B′). **(C, C′, C″)** Root surface of *Fgf23*$^{-/-}$ (2C′) mice compared to WT (2C) and Hyp (2C″). Note lack of a clear demarcation between dentin and cementum in the *Fgf23*$^{-/-}$ (2C′) and the *Hyp* (2C″) mice. **(D, D′, D″)** TEM analysis of root surface of *Fgf23*$^{-/-}$ (2D′) mice compared to WT (2D) and Hyp (2D″). Note lack of fibrillar structure in the *Fgf23*$^{-\backslash-}$ mice and a lack of a clear demarcation between dentin and cementum in the *Fgf23*$^{-/-}$ (2D′) and the *Hyp* (2D″) mice even under high magnification.

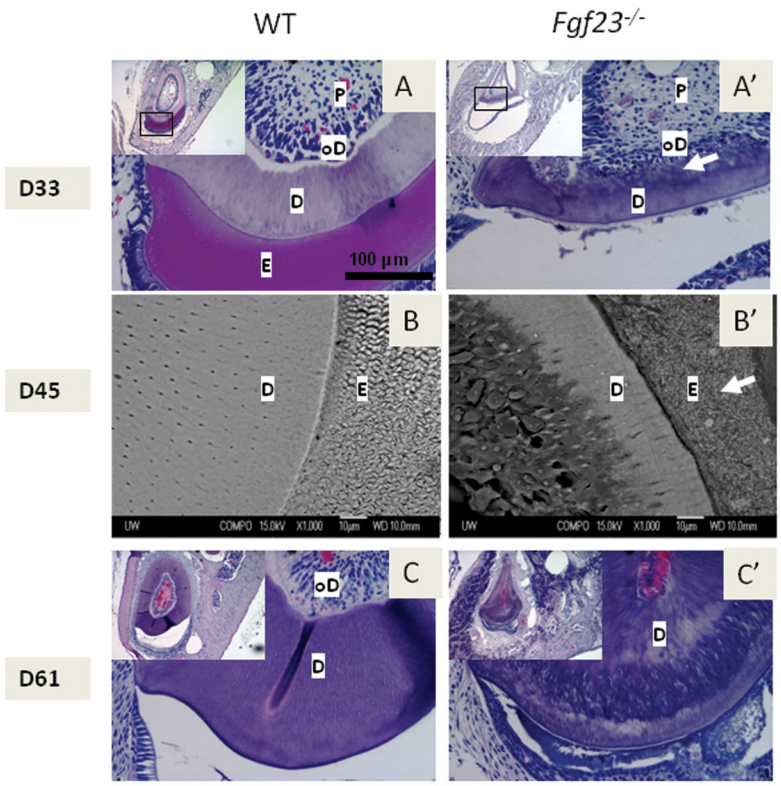

Figure 3. Mandibular incisors of *Fgf23*$^{-/-}$ mice exhibit dentin and enamel abnormalities

Representative H&E stained histological sections from mouse molars at 33 and 61dpc and SEM images from 45dpc incisors (At least three samples from each age and genotype were evaluated). P=pulp, oD=odontoblasts, D=dentin, E=enamel

(A, A′) Cross section of *Fgf23*$^{-/-}$ mouse incisor (3A) compared to the WT (3A′) at 33dpc. Inset shows cross-sections of the entire mandible. Note large cyst-like structure in the *Fgf23*$^{-/-}$ section (inset), and cells embedded in the dentin of *Fgf23*$^{-/-}$ mouse incisors (white arrows). Absence of enamel matrix (stains pink in the WT) in the *Fgf23*$^{-/-}$ mouse suggests dysfunctional amelogenesis. **(B, B′)** SEM analysis of 45dpc WT and *Fgf23*$^{-/-}$ mandibular first molars and incisors. **(B)** WT incisor dentin with normal tubular structure and interwoven enamel rods. **(B′)** *Fgf23*$^{-/-}$ incisor dentin was hypomineralized on the labial aspect and multiple embedded cells could be seen, and enamel rod structure is lacking (arrow). **(C, C′)** Cross section of *Fgf23*$^{-/-}$ mouse incisor (3C′) compared to WT (3C) at 61dpc. Note almost complete obliteration of pulp chamber in the *Fgf23*$^{-/-}$ mouse incisor and lack of the cyst-like structure (observed in 33 and 45dpc tissues).

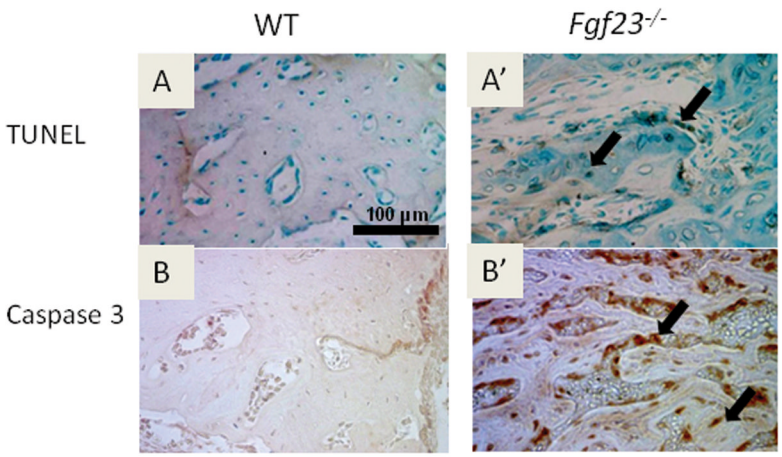

Figure 4. ***Fgf23*** $^{-/-}$ **mice exhibit increased apoptotic cells in the mandible compared to WT**

Histological sections from 45dpc mice (at least three of each genotype were used) were used to stain for **(A, A′)** TUNEL (dark brown stain) and **(B, B′)** Caspase 3 (red stain) to detect apoptotic cells. **(A′, B′)** Both stains indicated increased incidence of apoptosis in osteocytes and osteoblasts (arrows).

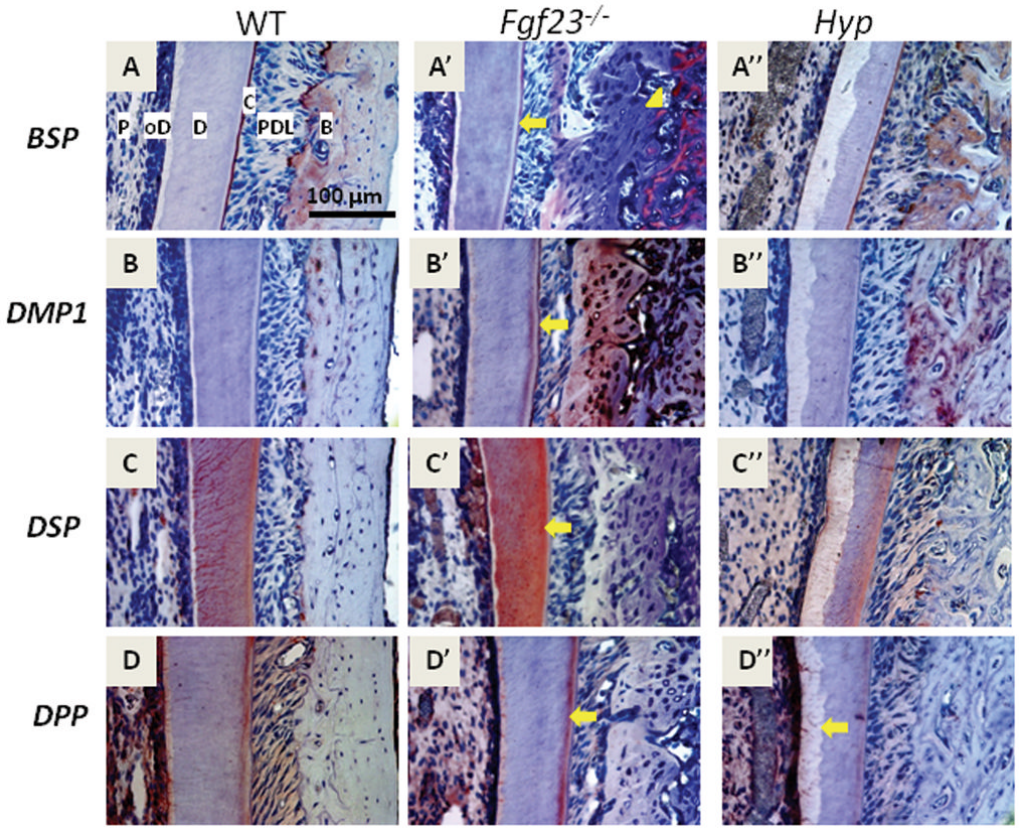

Figure 5. *Fgf23* ablation or *Phex* mutations cause altered expression of extracellular matrix genes and proteins of the oral mineralized tissues

Representative immunohistochemical images from the buccal side of the mandibular first molar at 45dpc (all antibodies were evaluated with at least three *Fgf23*$^{-/-}$, *Hyp*, and WT samples). Labels are provided in 5A for reference: P=pulp, oD=odontoblasts, D=dentin, C=cementum, PDL=periodontal ligament, B=bone

(A, A′, A″) *BSP* was localized to cementum and alveolar bone in WT and *Hyp* sections, whereas *BSP* was seemingly absent in *Fgf23*$^{-/-}$ alveolar bone directly adjacent to the PDL, strongly localized in the region associated with open osteocyte lacunae (5A′, arrowhead), and stained weakly in cementum (arrow) **(B, B′, B″)** ***D****MP1* staining was absent in cementum of WT and *Hyp* tissues, whereas *DMP1* was increased in mantle dentin, cementum (arrow), and bone in *Fgf23* $^{-/-}$ mouse tissues. *DMP1* was also increased in bone in *Hyp* mouse tissues (C′). **(C, C′, C″)** *DSP* was detected in the dentin tubules and mantle dentin of WT specimens (5C). *DSP* staining in *Fgf23* $^{-/-}$ dentin tubules was diffuse, but intensely localized to mantle dentin (5C′, arrow). *DSP* staining in *Hyp* dentin appeared lower, i.e. no clear staining in dentin tubules and sparse staining in the mantle dentin (5C″). **(D, D′, D″)** *DPP* staining detected at the predentin/dentin mineralization front, in odontoblasts and in mantle dentin of WT samples, and similarly localized in *Fgf23*$^{-/-}$ sections, but staining was stronger in the mantle dentin (5D′, arrow). *DPP* staining was weak in the mantle dentin of *Hyp* mice compared to WT, with no staining at the mineralization front (5D″, arrow).

Table 1

Summary of immunohistochemical staining of SIBLING members: bone sialoprotein, BSP; DMP1, dentin sialoprotein, DSP; dentin phosphoprotein; DPP

	WT	***Fgf23*$^{-/-}$**	***Hyp***
BSP	Acellular cementum and extracellular matrix (ECM) of bone	Decreased staining in acellular cementum, some areas of strong, localized staining in ECM of bone	Similar to WT, acellular cementum staining width thinner in *Hyp*
DMP1	Osteocytes and perilacunar bone	Increased staining detected in acellular cementum, mantle dentin, osteocytes, and bone ECM	Staining detected in osteocytes, perilacunar bone, and more widely in bone ECM
DSP	Staining in dentin confined to dentin tubules and mantle dentin	Strong, diffuse staining in tubules and mantle dentin	No apparent staining in dentin tubules, some staining in mantle dentin
DPP	Staining detected in odontoblasts, mineralization front between dentin and predentin, and mantle dentin	Strong staining in mantle dentin, weak staining in odontoblasts and predentin/dentin mineralization front	Staining in odontoblasts, weak staining in mantle dentin, no staining at dentin/predentin mineralization front